# A Multi-Temporal Analysis of Archaeological Site Destruction using Landsat Satellite Data and Machine Learning, Moche Valley, Peru

NICOLE D. PAYNTAR, The University of Texas at Austin, USA

The destruction of archaeological sites and the loss of archaeological landscapes remains a global concern as populations and urban areas continue to expand. Archaeological sites are not only significant to local communities, national identities, and modern tourist economies but also provide critical knowledge of past sociocultural interactions, settlement patterns, human-environment relationships, and risk mitigation strategies. While archaeological landscapes and site destruction have remained outside of traditional land use land cover change (LULCC) studies, they are a form of urban and agricultural land use. By conceptualizing archaeological site destruction within land change science, this study provides an innovative approach for assessing "what's left" of historically surveyed archaeological landscapes. Using a Random Forest algorithm and Landsat satellite data, this study quantifies archaeological site destruction attributed to LULCC in Peru's lower Moche Valley between 1985 and 2020. More than 400 archaeological sites previously recorded during the Chan Chan-Moche Valley Project (CCMVP, 1969–1974) are analyzed. Results indicate that less than a quarter of the original CCMVP sites remain on the landscape. The primary drivers of LULCC in the lower Moche Valley include population growth, migration, and government policies, while secondary drivers include heritage values. Positioning archaeological survey data within land change science and integrating machine learning techniques can benefit historic survey reassessments globally and provides significant knowledge of archaeological site destruction and the socioeconomic conditions that underly dynamic landscape changes.

CCS Concepts: • **Computing methodologies** → *Machine learning*; *Supervised learning by classification* • **Applied computing** → *Archaeology*;

Additional Key Words and Phrases: Land-use change, remote sensing, machine learning, archaeology, heritage, Peru

**ACM Reference format:**
Nicole D. Payntar. 2023. A Multi-Temporal Analysis of Archaeological Site Destruction using Landsat Satellite Data and Machine Learning, Moche Valley, Peru. *ACM J. Comput. Cult. Herit.* 16, 3, Article 47 (August 2023), 20 pages.
https://doi.org/10.1145/3586079

## 1 INTRODUCTION

Archaeological ground surveys are critical to identifying archaeological sites and the material remains of past cultures and peoples. They are the precursor to conservation and preservation initiatives, tourism development, scholarly excavation, and academic research. Archaeological survey is also the antecedent for public and private development and the transition of past landscapes to modern agricultural, industrial, or residential use. Since the early 20th century, scholars and **cultural resource management** (**CRM**) professionals have conducted surveys at a global scale. The majority of this work has focused on undeveloped and previously un-surveyed areas. Routine follow-up surveys are rare, creating a gap in how scholars and CRM professionals address "what's left" of archaeological landscapes where historic surveys (i.e., surveys more than 50 years old) were completed.



Author's address: N. D. Payntar, Department. of Anthropology, University of Texas at Austin, 2201 Speedway, Austin, TX 78712.

1556-4673/2023/08-ART47
https://doi.org/10.1145/3586079

Alternative methods for reassessing archaeological sites identified by past ground surveys are limited. Resurveying landscapes is costly (e.g., field-housing, food, stipends) and constrained by time, weather, and the ability of personnel to physically ground-truth and access sites, which may be remote or located in difficult terrain. In some cases, sociopolitical conflicts prevent archaeologists from accessing previously recorded sites. Satellite remote sensing is a cost-effective option that has allowed archaeologists (and citizen scientists alike, e.g., GlobalXplorer) to examine and monitor archaeological sites from afar. While remote sensing is not a direct substitute for survey (see Study Limitations), the method presented here allows archaeologists to assess and consolidate what has survived on archaeological landscapes faster than traditional methods, to determine the drivers of site destruction, and to inform future ground-truthing, excavation, and conservation at remaining sites. Using Peru's lower Moche Valley as a case study, this article provides an innovative approach to reassess *known* archaeological landscapes by leveraging machine learning algorithms, remote sensing, and land change science to quantify archaeological site destruction and identify the drivers of **land use land cover change** (**LULCC**) that contribute to the loss of archaeological landscapes.

Remote sensing technologies and spatial resolution have rapidly progressed since the 1970s and the initial launch of the ERTS **Multispectral Scanner** (**MSS**) that was limited to 80-meter resolution [Fowler 2010]. Prior to this, archaeologists relied on aerial photographs that enabled significant contributions to early archaeological survey and land assessment [Kosok 1965; Miller 1957; Willey 1953]. Current high-resolution satellite data has allowed archaeologists to analyze urban encroachment [Moise et al. 2021; Vaz 2020; Elfadaly et al. 2018], wartime site destruction [Angiuli et al. 2021; Cunliffe 2014], site damage and looting [El Hajj 2021; Rayne et al. 2020; Caspari 2020; Masini and Lasaponara 2020; Cuca and Hadjimitsis, 2017; Parcak 2015] and to conduct archaeological prospection [Orengo et al. 2020; Casana 2020; Kempf 2019; Dawson et al. 2020]. Scholars have also made advances in modeling and quantifying land use in ancient societies [Loughlin et al. 2021, Stephens et al. 2019, Hughes et al. 2018], utilizing deep learning to identify archaeological features [Karamitrou et al. 2022; Olivier and Verschoof 2021; Zingman et al. 2016], linking ancient land use and modern deforestation practices [Plekhov et al. 2021], and assessing site distribution and settlement patterns [Van Valkenburgh et al. 2020; Thompson 2020; Wernke et al. 2020]. Related to the current study, the ground-assessment and ethnographic research on urbanization and its impact on six archaeological sites in Trujillo, Peru by Gamboa [2016] provides insight into the experience of local communities and heritage management. Studies incorporating LULCC (i.e., land change science) and spatial computation methods for archaeology remain limited [Agapiou 2021; Nebbia et al. 2021]. While the use of satellite imagery for archaeological research is not a new phenomenon, the integration of land change science and the conceptualization of archaeological survey data within this broader framework is the major contribution of this article. By integrating archaeological survey with LULCC, remote sensing, and machine learning, a deeper understanding of the primary and secondary drivers of archaeological destruction, and the complex human-environment interactions and socioeconomic policies that underly these changes, is possible.

*Land cover* refers to the surface cover on the ground (e.g., vegetation, asphalt, open water, bare soil) whereas *land use* refers to how a landscape is used (e.g., residential, agriculture, industrial) [Tewabe and Fentahun 2020]. Knowing and quantifying what land-use types are present–and when–can help address the destruction of archaeological landscapes over time. Land change drivers are often difficult to link empirically because they depend on dynamic spatiotemporal variables [Turner et al. 2007]. Previous research has shown, however, that national policies and governance, population growth, global commodity value chains, foreign investments and the acquisition of land, new technologies, migration, labor availability, climate change, and so forth are all potential land change drivers [Zimmerer and Vaca 2016; Meyfroidt et al. 2013; Hecht 2010; Turner et al. 2007].

Traditional studies of LULCC include the expansion of agriculture and urbanization, biodiversity loss, deforestation, carbon emissions, and the effects of land change on ecosystem services [Lambin and Meyfroidt 2011; Rudel et al. 2009; Huston 2005; Rindfuss et al. 2004; Geist and Lambin 2002]. Recent advances in machine learning have increased LULCC classification accuracy [Rahman et al. 2020; Vega Isuhuaylas et al. 2018], leading to high-resolution object segmentation [Wang et al. 2021; Zarro et al. 2020] and the analysis of geospatial big data

[Li et al. 2021; Kalantar et al. 2020]. This knowledge is used to develop strategies to conserve fragile ecosystems, resolve socioeconomic pressure, and develop sustainable land management solutions. In Peru, extensive LULCC research has been conducted on deforestation and biodiversity loss [Álavarez-Berríos et al. 2021; Vargas et al. 2019; Bax et al. 2019], agricultural expansion [Sánchez-Cuervo et al. 2020; Gutiérrez-Vélez et al. 2011; Tovar et al. 2013], urbanization and infrastructure development [Ramierez et al. 2019], crop classification [Tatsumi et al. 2016], and mining [Cabellero Espejo et al. 2020; Asner and Tupayachi 2017].

While archaeological landscapes have remained outside of traditional LULCC studies, they are a form of urban and agricultural use and provide valuable cultural ecosystem services (e.g., tourism revenue, heritage values, and cultural identity [Tengberg et al. 2012]). The inclusion of archaeological landscapes within a broader LULCC framework is applicable for four reasons. First, the loss of archaeological landscapes is physically measurable using archaeological survey data and remote sensing. Landscape loss can also be measured economically (e.g., tourism revenue) and correlates to sustainable practices (both socioeconomic and in terms of archaeological preservation). As Eric Vaz [2020, p. 2] argues, the "preservation of archaeological sites allow sustainable landscapes to be supported, particularly within small towns that rely on product differentiation, seasonal tourism, and endogenous economies…". Second, similar to biodiversity loss, land-use change significantly affects diverse representations of the past and modifies access to cultural resources, amplifying identity and heritage erasure. In the past, it has been difficult to analyze the erasure of cultural ecosystem services because of their intangible properties [Bürgi et al. 2017]; however, quantifying archaeological site destruction can provide insight into fluctuating cultural values. Third, adopting a LULCC framework provides archaeologists with a more comprehensive understanding of the dynamic nature of landscape change and archaeological site destruction. Finally, the conversion of archaeological landscapes to new land-use classes (e.g., agriculture, industrial, urban) influences natural resource exploitation, carbon emissions, and local carrying capacity. The current study focuses on the first three factors. Knowing what remains of archaeological landscapes and the causal factors associated with archaeological destruction is beneficial to researchers, NGOs, and government agencies who influence policy decisions and conservation initiatives worldwide.

This article utilizes computational methods to quantify archaeological site destruction and integrates archaeological survey data with machine learning, land change science, and remote sensing to provide an innovative and cost-effective approach to assess what remains of historically surveyed archaeological landscapes. A Random Forest algorithm and Python is used to classify 35 years of Landsat satellite imagery in Peru's lower Moche Valley (1985–2020). A total of 477 archaeological sites recorded during the **Chan Chan-Moche Valley Project** (**CCMVP**, 1969-1974) are analyzed. LULCC is assessed at both the regional and the site scale. The goal of this research is to (1) provide an innovative approach to archaeological LULCC change that can be scaled globally to assess surveyed archaeological landscapes, (2) convey a broader understanding of the long-term impacts of socioeconomic policies and heritage discourse that contribute to the loss of archaeological landscapes in Peru, and (3) to identify remaining CCMVP archaeological sites in Peru's lower Moche Valley.

## 2 MATERIALS AND METHODS

### 2.1 Case Study: Lower Moche Valley, Peru

Located along Peru's arid North Coast and situated in the department of La Libertad, the Moche Valley is home to the country's third largest city—Trujillo—with an estimated urban population of more than 1.4 million people [INEI n.d.]. Agrarian land reforms in the 1970s and Peru's neoliberal policies in the 1990s globalized and expanded the country's exports making the Moche Valley the largest commercial sector in the La Libertad province [Velarde 2018; Schwarz and Mathijs 2017; Schuster and Maertens 2016]. Under these policies, the region became a leading producer of footwear, sugar cane, asparagus, blueberries, mango, and avocado, to name a few [Apaz et al. 2019]. Today, the Moche Valley retains significant agro-industrial status, with most arable coastal land having been acquired by domestic and international corporations from small-holding agricultural communities [Thompson et al. 2016]. To sustain agro-industrial and residential growth, irrigation has been critical. The Chavimochic Irrigation Project diverts water from the neighboring Santa Valley to support 78,310 hectares of land in the Moche Valley as well as the expansive urban and agricultural growth of Trujillo and its outlying districts [Mark et al. 2017; World Bank 2021]. Evidence of pre-historic canal systems—some of which are still in use today—is also found throughout the region, underlying the significance of water management both past and present [Caramanica et al. 2020; Huckleberry et al. 2012; Billman 2002; Ortloff et al. 1985; Farrington and Park 1978]. The region is, however, highly susceptible to catastrophic **ENSO** (**El Niño Southern Oscillation**) events, which periodically disrupt agro-industrial production and land use due to widespread flooding and infrastructure damage [Ráez Luna 2017].

The Moche Valley also has a rich archaeological history with numerous pre-ceramic lithic sites and the built remains of several state and imperial cultures including the Moche (100–700 CE), Chimú (900–1470 CE), and Inca (1470–1532) [Quilter 2021; Prieto et al. 2019; Vogel 2018; Chapdelaine 2011; Moore and Mackey 2008; Castillo and Uceda 2008; Moseley 2001; Shimada 2000; Moseley and Cordy-Collins 1990; Mackey 1982; Moseley and Mackey 1972]. Archaeological tourism has steadily increased over the past decade, providing income for local artisans and hospitality workers [Dupeyron 2021; Coben 2014; Underberg-Goode 2014]. Recent government investment, infrastructure development, and the promotion of the *Ruta Moche* tourist circuit are partly responsible for rising visitor rates. For example, visitors to the archaeological complex of Huaca del Sol y de la Luna increased from 98,143 in 2009 to 136,653 in 2019, an increase of roughly 40% (MINCETUR). The *Ruta Moche* includes the UNESCO World Heritage Site of Chan Chan, the national patrimonial sites of Huaca de la Luna y Huaca del Sol, and El Brujo, as well as several sites located outside of the Moche Valley [Underberg-Goode 2014]. The majority of tourists visiting Peru, however, remain disproportionately concentrated in the former Inca capital of Cuzco and its surrounding region.

### 2.2 Archaeological Data and Archival Records

The archaeological dataset used in this study consists of 477 archaeological sites previously recorded during the CCMVP (1969–1974), co-directed by Michael Moseley and Carol Mackey. It should be noted that the CCMVP sites do not represent the totality of archaeological sites in the Moche Valley, but only a fraction of the total. The digitized locations of all sites from the original CCMVP documentation were generously provided by Brian Billman (UNC-Chapel Hill) and Patrick Mullins (University of Pittsburgh) as part of the **Moche Valley Ancient Settlement Database** (**MVASD**) to enable QGIS compatibility. Site locations are represented as point data (e.g., a site's center). The author ground-verified a 10% sample of all CCMVP sites to assess the accuracy of site geolocations and to record common land-use practices adjacent to sites in 2018. For sites that were still present on the landscape, geolocation accuracy fell within 7–10 m of digitized points.

Archival work was conducted by the author at the Harvard Peabody Museum Archives to access the "Michael E. Moseley Papers on the Chan Chan-Moche Valley Project" in 2019. CCMVP field notes define a wide range of identified sites including middens, platforms, burials, canals, roomed structures, and large ceramic sherd scatters. The majority of recorded sites were attributed to the Moche, Chimú, and Chimú-Inca periods. Notes recorded by Ian Farrington (Nov. 1–7, n.d.) and Charles M. Hastings (March–May 1973) detail the material remains of identified sites as well as nearby land-use practices:

> "Some of the so called structures must have been so but during later occupation of the pampa they were almost destroyed leaving just *rectilinear patterns of rocks, wall footings etc. with sherds.*" (Farrington, n.d.; author's emphasis)

> "The survey in this area has taken on a very real air of salvage archaeology. More than 50% of the sites which appear on the 1942 photos have been completely destroyed; so much land has been reclaimed for agriculture in the past few decades that generally *only the sites in marginal locations survive.*" [Hastings, 1973; author's emphasis]

> "Forty strong possibilities were gone without a trace; *the most common cause of destruction is the reclaiming of land for agriculture, but building construction, roads, and canals are also factors.* I recorded only two sites. One is a midden with little architecture and poor preservation and *the other a destroyed structure with a worthwhile sample of sherds scraped to one side of the site.* Both sites are either late Moche and/or Early Chimu." [Hastings, 1973; author's emphasis]

Observations made by Hastings and Farrington regarding disturbed stone structures, large ceramic scatters, and the marginal locations of surviving sites are similar to the author's own observations during ground verification.

For the purposes of this study, sites identified between 1969 and 1974 are considered present on the landscape during the entirety of the CCMVP, despite reports of landscape development detailed by Hastings and other project members while surveying. This leaves an unavoidable 11-year gap between the last CCMVP survey date and the 1985 Landsat 5 Thematic Mapper satellite data (Landsat 2 imagery prior to 1985 remains unusable; see Landsat Time-series Data). While it is not possible to calculate LULCC rates within this 11-year period, it is possible to infer which CCMVP sites were likely to have been destroyed prior to 1985 based on the algorithms classification of land use in 1985.

### 2.3 Landsat Time-Series Data

To quantify archaeological destruction and identify the primary drivers of LULCC in the lower Moche Valley, Landsat multispectral satellite images were collected at 5-year intervals (path 009, row 066) with WGS84 datum, projection UTM Zone 17S, and spatial resolution of 30 × 30 m per pixel from 1985 to 2020. Landsat's open source availability and time-series depth make it valuable and cost-effective for LULCC analysis. Data quality, however, becomes more variable with earlier sensors. Although Landsat 2 images were available prior to 1985, the data quality and resolution remained too low to include in the current analysis. Landsat 5 Thematic Mapper tiles were collected for 1985, 1990, 1995, 2000, 2005, and 2010 while Landsat 8 OLI/TIRS tiles were collected for 2015 and 2020. Images from Landsat 7 were bypassed in favor of Landsat 5 tiles during collection due to an error in the Line Scan Corrector after 2003 [Young et al. 2017]. All satellite images were downloaded from **United States Geological Survey** (**USGS**) Earth Explorer Collection 2 Level 2, which is calibrated for surface reflectance. The study area encompasses 115,535 hectares across the lower Moche Valley.

### 2.4 Geospatial Data Extraction

LULCC were selected based on the author's ground-verification field work, visual interpretation of the Landsat data, CCMVP archival materials, and Google Earth images. In total, seven classes were selected: Desert/Barren, Water, Poultry Farming, Urban, Roads, Agriculture, and Mountain Scrub. Here, Agriculture is defined as active and fallow fields and also includes vegetation categories like parks, gardens, and so forth. Although Roads are traditionally classified as a subset of Urban land use, the two classes were separated for this study based on archival records indicating the rapid expansion of roadways between 1970 and 1974. Clouds were trained as an eighth class to assess the percent of cloud cover per year in each Landsat image.

An ALOS World 3D–30 m **Digital Surface Model** (**DSM**) was used to calculate elevation and slope rasters for the study area. A DSM was selected instead of a **DEM** (**Digital Elevation Model**) based on the relatively flat coastal topography of the lower Moche Valley. The DSM provides elevation measurements from the top of buildings, vegetation, and so forth, rather than ground level (DEM). **Normalized Difference Vegetation Index** (**NDVI**) was also calculated for each study year. Landsat bands 1–7 were used to create a composite image for Landsat 8 OLI/TIRS and Bands 1–6 were used for Landsat 5 TM. Individual Landsat composite images were then stacked with their corresponding NDVI rasters, elevation, and slope rasters.

For each Landsat satellite image, polygons representing the eight LULCC classes were produced by the author using QGIS—a free and open source platform for geographic information system applications and analysis of geospatial data. Four hundred pixels per class (3,200 pixels total) were randomly sampled within each polygon.

This was repeated for each Landsat image and polygon set. Point Sampling was then utilized to extract underlying polygon attributes and raster values from the stacked raster layers (e.g., NDVI, elevation, slope). This data was exported and used to train a **Random Forest** (**RF**) algorithm using Scikit Learn and Python. The addition of the NDVI, slope, and elevation raster layers enabled the RF algorithm to learn subtle differences between each land-use class and further differentiate pixel values in tandem with the Landsat bands. The method outlined here can be utilized globally by tailoring land-use classes based on specialist knowledge of different regions and study areas.

### 2.5 RF Algorithm

RF was selected because of its unparalleled accuracy and its ability to run efficiently on large datasets [Doyle et al. 2021; Sánchez-Cuervo et al. 2020; Tatsumi et al. 2016; Kulkarni and Lowe 2016]. RF is a supervised machine learning algorithm that develops large numbers of decision trees to classify sets of variables [Breiman 2001]. The goal of a decision tree classifier is the separation of groups at each non-terminal node and the choice of features that are most effective in distinguishing the class grouping [Kulkarni and Lowe 2016]. The decision trees are aggregated to provide the average of the individual tree outputs.

Training data consisted of 400 pixels per class (3,200 pixels total per year) with 70% of individual pixel classes used for training and 30% of each pixel class withheld for validation. Previous studies have demonstrated the 70–30% split generates the lowest mean standard error and best model performance when compared to other split options [Nguyen et al. 2021; Adelabu et al. 2015]. An **Out-of-Bag** (**OOB**) score was generated to assess RF model accuracy and error rate from the reserved validation data. The OOB estimate is derived from the classification error for the samples omitted from each tree, which is averaged over the total number of trees [Tatsumi et al. 2016]. GridSearchCV was utilized to test the two hyperparameters that have the greatest impact on algorithm accuracy—max_depth and n_estimators [Doyle et al. 2021]—and optimize the RF models. n_estimators refer to the number of trees created while max_depth is defined as the number of levels in each tree. Value combinations for all n_estimators (5, 10, 50, 100, 250, 300, 350) and max_depth (2, 4, 8, 16, 32, 64, None) were tested for each year of the study. This resulted in 49 RF models per year and a total of 392 RF models spanning 1985–2020. For each year, the RF model with the highest validation accuracy and lowest OOB error rate was selected, resulting in the eight models used in this study.

Additionally, sites ground-verified by the author in 2018 were compared to the 2020 RF land-use classification to generate a confusion matrix and further assess destruction accuracy and the algorithms precision, sensitivity, and specificity scores. Despite a 2-year difference between the 2020 RF model and on-site ground verification, the 40 sites selected were located in marginal areas where land-use change was largely stable when comparing the 2015 and 2020 RF models. This is further evidenced by land-use majorities remaining the same in 2015 and 2020. Of the 40 sites ground-verified in 2018, 17 were inaccessible due to their location on private property; however, the surrounding land use was recorded and utilized for this additional accuracy assessment.

### 2.6 Extracting and Calculating LULCC

All classified raster images were exported to QGIS. The total area of each class was calculated per year before calculating the percent change of land use and land cover across the study region.

Following regional calculations, CCMVP sites were overlaid onto all classified raster images. A 50-m circular buffer was generated around all CCMVP sites (represented as point data) to extract representative land-use pixel values and quantify archaeological destruction per year. The selection of the 50-m buffer was based on CCMVP field notes describing site extents. While the author was unable to analyze the entirety of the CCMVP archival collection, the largest site estimate found by the author was attributed to Survey H38550: "The area covered by sherds was a square about 50-meters on a side, marked by linear boulder piles…" (Survey H38550). Although the extent of H38550's surface material is larger than other sites recorded by CCMVP surveyors, 50 m was selected as the maximum site extent for all CCMVP buffers to capture broader patterns of land use. Zonal Statistics were

Table 1. Reports n_estimators and max_depth as well as Model Accuracy (Rounded to the Nearest Whole Number) and OOB Measurements for the Eight RF Models used in this Study

| Landsat Satellite | Year | n_estimator | max_depth | Accuracy (%) | OOB |
|---|---|---|---|---|---|
| Landsat 8 OLI/TIRS | 2020 | 350 | 16 | 95 | 94.6 |
| | 2015 | 250 | None | 95 | 94.4 |
| Landsat 5 Thematic Mapper (TM) | 2010 | 250 | 32 | 96 | 96.1 |
| | 2005 | 250 | 16 | 95 | 94.8 |
| | 2000 | 250 | 32 | 95 | 94.2 |
| | 1995 | 100 | 32 | 94 | 94.1 |
| | 1990 | 350 | 16 | 96 | 96.8 |
| | 1985 | 250 | None | 97 | 96.2 |

used to extract the majority land-use class represented within individual site buffers. These values were then exported to determine land-use change and destruction at the individual site scale.

Three tiers of destruction probability were determined based on land-use and transition patterns over time: High (urban, agriculture, road, water), Medium (poultry farm), and Low (desert/barren, mountain scrub, cloud). A site was considered destroyed if the majority land use within the 50-m buffer was identified as a High or Medium destruction category or if the site transitioned to one of these destruction tiers between 1985 and 2020. Sites that remained in the Low destruction categories between 1985 and 2020 are considered surviving sites on the landscape.

## 3 RESULTS AND ANALYSIS

### 3.1 RF Accuracy Assessments and Algorithm Runtime

RF training accuracy scores for Landsat 8 OLI/TIRS models averaged 94.5%, whereas accuracy for Landsat 5 TM models ranged from 96.8 to 94.1% based on OOB values. Table 1 reports RF accuracy measurements of the eight selected models for each study year. Overall, algorithm validation accuracy was high with an average score of 95.1% across all models. Additionally, a confusion matrix for the 2020 RF model was generated to compare the RF algorithms land use classifications and the author's ground-verification observations recorded at 40 CCMVP sites in 2018 to assess the algorithm's accuracy predicting site destruction (Figure 1). The classifier's overall accuracy when determining site destruction was 80% with an error rate of 0.20. The classifiers sensitivity (0.90), precision (0.56), and specificity (0.76) measurements were generally high. For these three measurements, the closer a score is to 1, the stronger the result. Finally, the classifier's false-positive rate was low with a value of 0.23 (a score closer to 0 is considered strong).

The majority of classification inaccuracies for Landsat 8 OLI/TIRS and Landsat 5 TM models were attributed to the separation of Roads from the Urban class and vice versa. This is understandable given the resolution of the Landsat imagery and considering that Roads are traditionally a subclass within Urban land use. Additionally, the algorithm's ability to distinguish between Desert/Barren and Poultry Farms was noticeably weaker than other land-use classes despite the inclusion of the DSM. In the Moche Valley, poultry farms are located almost exclusively in desert areas and inherently include desert within their footprint, as each building on a given property is separated by sandy, barren land. The relatively small size of Poultry Farms and the inability to distinguish individual buildings given the 30-m resolution made training for this class difficult. Small discrepancies were also noted between Mountain Scrub and the Desert/Barren categories due to variations in sediments, seasonal gullies (channels that form following heavy rainfall and deposit sediment), and shadows attributed to cloud cover. These classification discrepancies were manually corrected by the author during post-processing using the **Semi-Automatic Classification** (**SCP**) tool in QGIS.

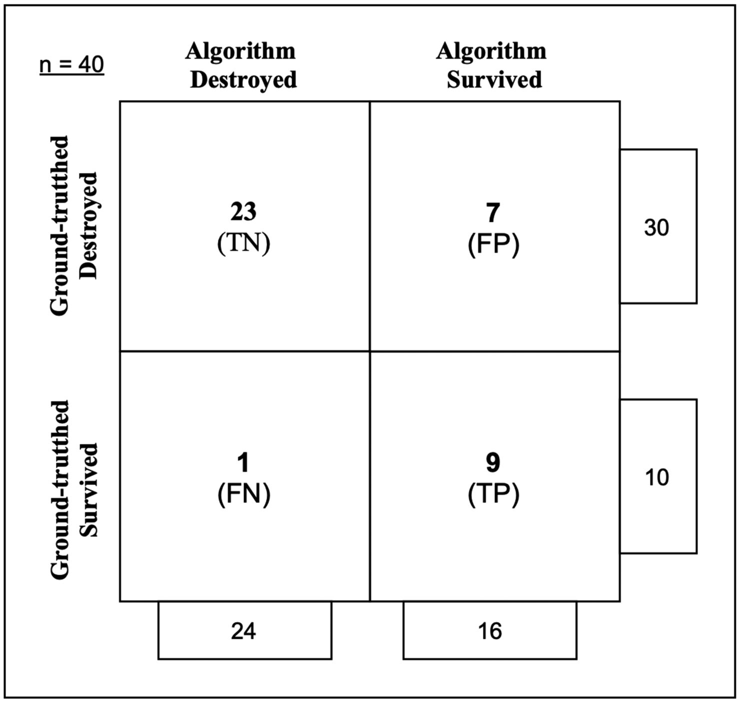


Fig. 1. Site destruction confusion matrix. A confusion matrix was generated to compare sites ground-verified by the author vs. the RF 2020 models accuracy when classifying site destruction or survival based on land use.

The average runtime for testing all combinations of n_estimators and max_depth for RF optimization was 3 min 51 sec, while the algorithm's total runtime to classify satellite imagery for the eight selected RF models was 22 min 52 sec. Post-processing, pixel reclassification, and data extraction was estimated to be 72 h. For comparison, the author was able to visit an average of six sites per day with an estimated daily hiking range of 8–11 miles while ground-verifying site destruction and land use in 2018. Depending on the condition of individual sites, an average of 1 h 16 min was spent recording ground observations (not including hiking time to access sites). In total, 40 CCMVP sites were visited during a 2-week period. The algorithm's ability to efficiently classify land-use patterns surrounding the 477 CCMVP sites in less than 25 min significantly outperforms the time required for physical site visits.

### 3.2 LULCC in Peru's Moche Valley

Figure 2 represents the total area (hectares) attributed to each land-use class between 1985 and 2020, whereas Figure 3 visually represents LULCC across all eight RF models. Between 1985 and 2020, poultry farms accounted for a 1,918% increase in land use—the highest percent change within the seven land-use classes. Roads increased by 227%, as did urban development (124%), and agricultural land use (19%). As poultry farms, agriculture, roads, and urban areas increased desert/barren and mountain scrub simultaneously decreased by 16% and 18%. The latter two land-use classes, however, still constitute the largest percentage of total land area, accounting for more than 60% (73,146 ha) of undeveloped land within the 115,535 ha study zone as of 2020. By comparison, agriculture accounted for 13% (14,784 ha) of total land area, and urban areas and roads formed a combined 10% (13,135 ha) of total land area by 2020 (Figure 2).

Cloud coverage within individual Landsat images averaged less than 2% across all study years with the exception of 2010. The presence of clouds was contained to the mountainous regions east of Trujillo, at the outer

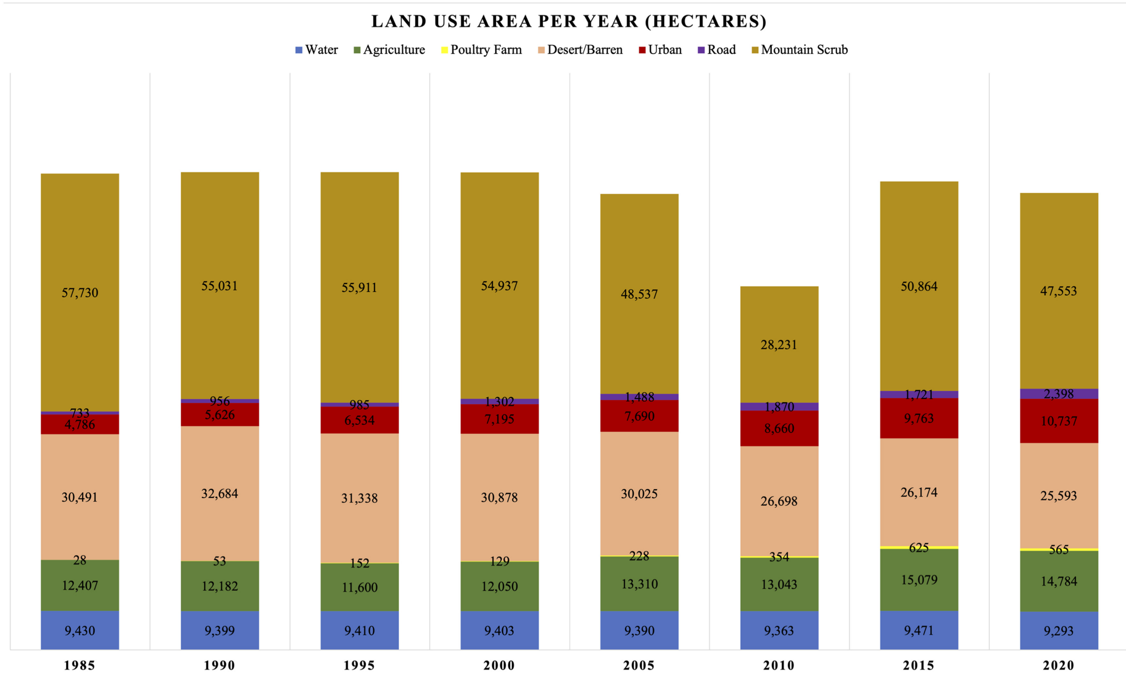


Fig. 2. Land-use area per year (hectare). Land-use change in Peru's lower Moche Valley represented in hectares. Cloud cover is not included but accounts for the variations in the Mountain Scrub land-use area in 2010.

Table 2. Variety of Identified Land-Use Classes in 50-m Site Buffers

| | Variety of Identified Land Use Classes in 50m Site Buffers | | | | | | |
|---|---|---|---|---|---|---|---|
| | **1985** | **1990** | **2000** | **2005** | **2010** | **2015** | **2020** |
| **# Sites One Land Use Class** | 414 | 409 | 379 | 369 | 344 | 339 | 339 |
| **# Sites Two Land Use Classes** | 57 | 65 | 94 | 99 | 115 | 130 | 119 |
| **# Sites Three Land Use Classes** | 6 | 3 | 3 | 9 | 18 | 8 | 19 |
| **# Sites Four Land Use Classes** | 0 | 0 | 1 | 0 | 0 | 0 | 0 |

The number of land-use classes within individual 50-m site buffers are tabulated here. Sites represented by a single land-use class are most prominent in 1985. Single land-use homogeneity decreases moving toward the present as land use become more complex.

limits of the study area which are largely undeveloped. Despite 15 sites being covered by clouds in 2010 (as well as 1 site in 2005), clouds did not negatively affect land-use outcomes or the quantification of site destruction, as the sites in question were located in undeveloped mountain scrub. Notably, Landsat images from 1990 and 1995 do not include any cloud cover.

## 3.3 LULCC at CCMVP Sites

The creation of 50-m buffers surrounding individual CCMVP sites revealed the variety of land use occurring at sites, the total number of sites attributed to a land-use class per year, overall site destruction rates, and a timeline of site destruction.

Table 2 shows the diversity of representative land-use classes recorded within buffer zones for each study year. More than 70% of CCMVP site buffer zones could be attributed to a single representative land-use class, although, land-use homogeneity within archaeological buffers decreased over time. The year with the highest percentage

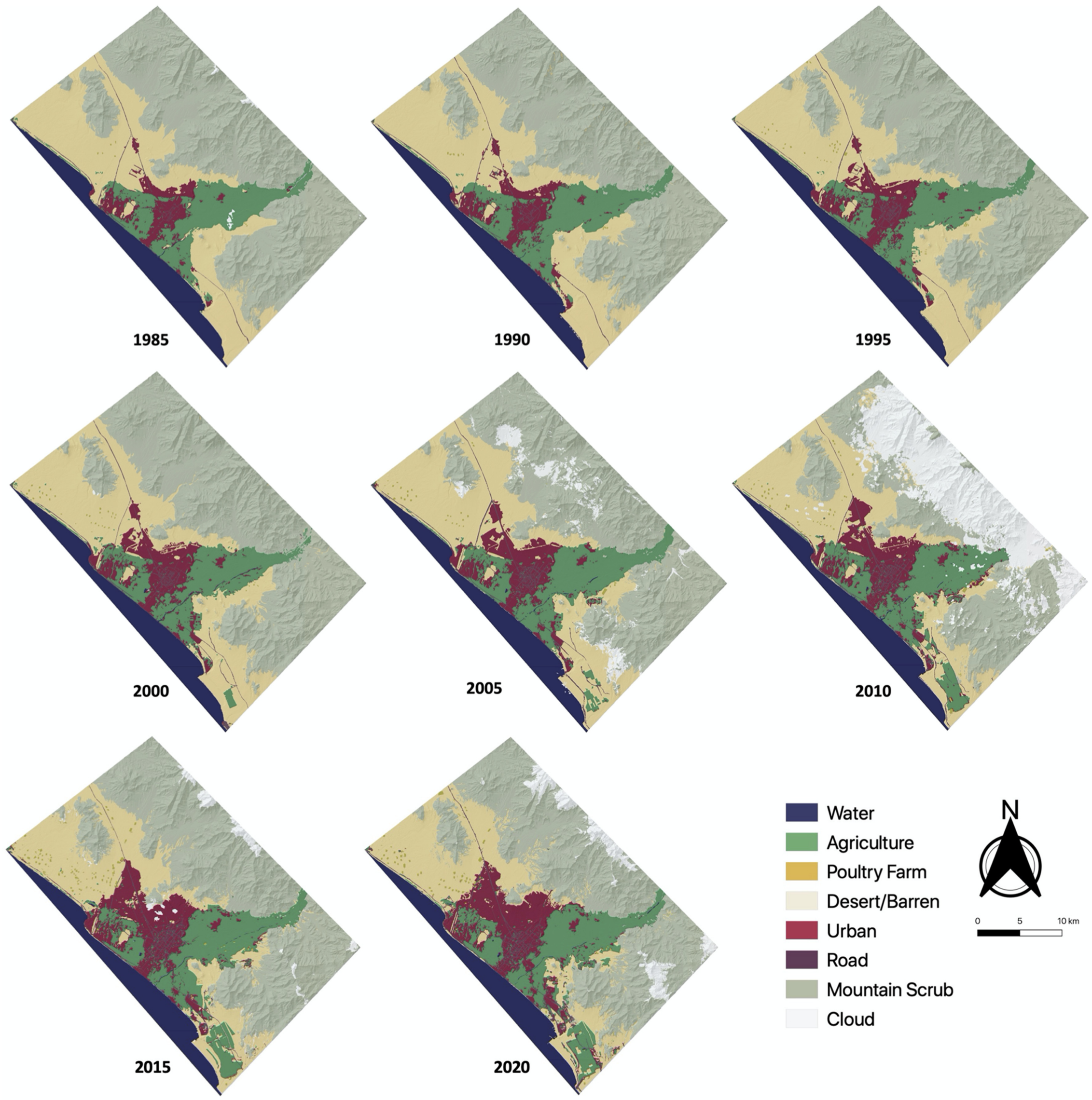


Fig. 3. Land-use change between 1985 and 2020 in Peru's lower Moche Valley.

of sites represented by a single land-use class was 1985. Roughly 86.8%, or 414 sites fell within one class. The year with the lowest number of sites with a single land use was 2020, with 71.1% or 339 single land-use sites. Decreased land-use homogeneity reflects the ongoing development and expansion of industrial, residential, and agricultural assets in the lower Moche Valley.

For sites that did not maintain a single land use over time, the majority land-use class was determined by the total area a class occupied within the 50-m buffer. The majority class was considered to be the representative land use at sites with two or more recorded land-use classes. The number of sites represented by two land-use classes ranged from 57 sites in 1985 to a high of 130 sites in 2015. Less frequently observed were sites represented

Table 3. Number of Sites within Land-Use Majorities

| | **Number of Sites within Land-Use Majorities** | | | | | | | |
|---|---|---|---|---|---|---|---|---|
| n = 477 | **1985** | **1990** | **1995** | **2000** | **2005** | **2010** | **2015** | **2020** |
| **Water** | 0 | 0 | 0 | 1 | 2 | 1 | 0 | 0 |
| **Agriculture** | 107 | 114 | 106 | 115 | 123 | 128 | 125 | 124 |
| **Poultry Farm** | 1 | 1 | 4 | 0 | 1 | 0 | 3 | 6 |
| **Desert/Barren** | 257 | 231 | 240 | 203 | 174 | 136 | 120 | 94 |
| **Urban** | 40 | 66 | 75 | 118 | 123 | 154 | 178 | 193 |
| **Roads** | 1 | 5 | 7 | 4 | 14 | 11 | 13 | 15 |
| **Mountain Scrub** | 71 | 71 | 45 | 36 | 39 | 32 | 38 | 45 |
| **Cloud** | 0 | 0 | 0 | 0 | 1 | 15 | 0 | 0 |

Land-use majorities were calculated for each 50-m site buffer. The number of sites per year occupying a majority land-use class are shown here.

Table 4. Number of Sites Destroyed per 5-Year Period

| | **Number of Sites Destroyed Per 5-Year Period** | | | | | | | | |
|---|---|---|---|---|---|---|---|---|---|
| | **1974-1985** | **1986-1990** | **1991-1995** | **1996-2000** | **2001-2005** | **2006-2010** | **2011-2015** | **2016-2020** | **Total Destroyed** |
| **Agriculture** | **107** | 15 | 5 | 8 | 8 | 8 | 4 | 4 | 159 |
| **Poultry Farm** | 1 | 1 | 4 | 0 | 0 | 0 | 0 | 1 | 8 |
| **Road** | 1 | 2 | 2 | 0 | 3 | 1 | 1 | 2 | 11 |
| **Urban** | 40 | **26** | **16** | **33** | **20** | **23** | **17** | **11** | **186** |
| **Total** | 149 | 44 | 27 | 41 | 31 | 32 | 22 | 18 | 364 |

Of the 477 CCMVP sites, 364 have been destroyed while 113 are estimated to remain on the landscape. Between 1974 and 1985, the highest rates of CCMVP destruction were recorded with a total loss of 149 sites. The land-use class attributed to the highest rate of archaeological destruction is urban expansion. Results in bold show the land-use class that destroyed the most sites per 5-year period.

by three or more land-use classes within the 50-m buffer zone. The number of sites with three land-use classes ranged from a low of 3 sites in 2000 to a high of 19 sites in 2020. Only one site in 2000 had four land-use classes recorded within the 50-m buffer zone—this was the maximum number of classes recorded for an individual site.

After determining the majority land-use class present at each CCMVP site, the total number of sites occupying individual land-use classes was calculated per year (Table 3). In general, the number of sites originally located in Desert or Mountain Scrub decreased after 1990 as land was simultaneously converted to agricultural or urban use. Notably, the number of sites consumed by urban land use steadily increased from 40 sites in 1985 to 193 sites in 2020. The land-use patterns detected at CCMVP sites are representative of the broader, regional trends reported in LULCC in Peru's Moche Valley.

## 3.4 CCMVP Site Destruction

Of the 477 sites recorded during the CCMVP, the current study reveals 364 sites have been destroyed, while 113 sites likely remain on the landscape (Figure 4). Surviving CCMVP sites are characterized by their remote locations to the north and east of Trujillo, in the coastal desert areas and the Andean foothills. As of 2020, 40 remaining sites are attributed to Mountain Scrub while 73 are located in the Desert/Barren land-use class. In total, more than 76.3% of CCMVP sites have been destroyed.

Table 4 shows the total number of sites destroyed per 5-year period as well as the land-use class attributed to destruction. The highest rate of archaeological destruction occurred between the end of the CCMVP survey and the first year of satellite coverage in this study. Between 1974 and 1985, 149 sites were destroyed. Of these, 107 sites were destroyed by agricultural expansion, 40 by urban development, 1 site by poultry farming, and

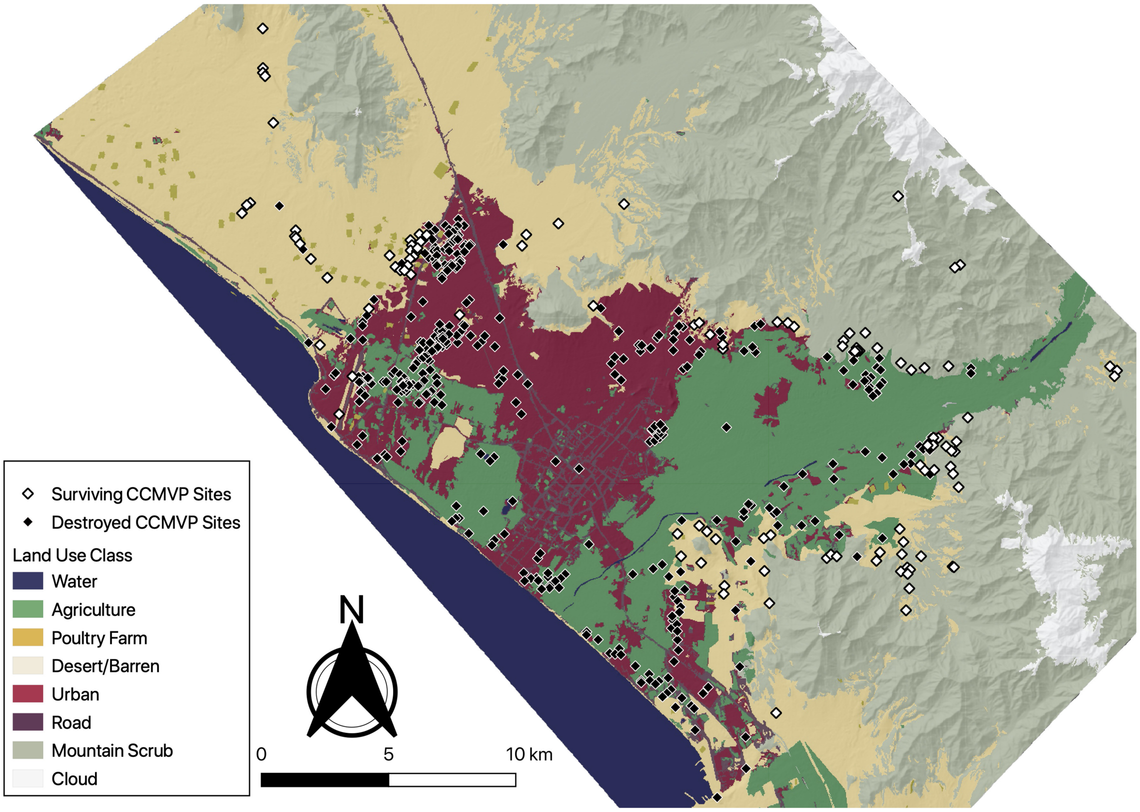


Fig. 4. Map of CCMVP site destruction. Of the 477 sites recorded during the CCMVP, 364 have likely been destroyed (High and Medium land-use destruction categories) while 113 have likely survived (Low destruction land-use categories).

1 site by roads. The second highest period of destruction (44 sites) occurred between 1986 and 1990, while the lowest destructive period (18 sites) occurred between 2016 and 2020. Moving toward the present, the lower rate of archaeological destruction is a circumstance of fewer sites remaining on the landscape. In extremely marginal landscapes this also raises questions about how representative archaeological survey data are, if surveys take place after significant periods of urban growth and agrarian expansion. Overall, destruction rates were relatively consistent from 1986 to 2020, with an average of 31 CCMVP sites destroyed per 5-year period.

Agriculture was the leading cause of archaeological destruction prior to 1985, but urban expansion quickly surpassed it. Between 1985 and 2020, urbanization accounted for a total loss of 186 CCMVP sites, while agricultural expansion was linked to the overall destruction of 159 sites and 11 sites were destroyed by road construction (Table 4). Despite poultry farms undergoing the largest percent change in land-use area over the 35-year period, only eight instances of CCMVP site destruction were attributed to this class.

# 4 DISCUSSION

## 4.1 Primary Drivers of Site Destruction

While many variables influence land-use change, the primary drivers of site destruction in the lower Moche Valley are population growth, migration, and government policies. Urbanization and agricultural expansion are the effects of these drivers, having played a major role in reshaping and erasing the archaeological landscape surrounding Trujillo and its outlying districts in the lower Moche Valley.

Table 5. Urban and Rural Population of La Libertad Province

| | Urban and Rural Population La Libertad Province | | | | | | |
|---|---|---|---|---|---|---|---|
| | **1940** | **1961** | **1972** | **1981** | **1993** | **2007** | **2017** |
| **Urban Population** | 122,177 | 246,847 | 474,465 | 631,529 | 870,390 | 1,184,548 | 1,403,555 |
| **Rural Population** | 273,056 | 351,078 | 326,512 | 350,545 | 399,871 | 432,502 | 374,525 |

Population data collected from the Institute Nacional de Estadística y Informática (INEI).

Table 6. Migration to La Libertad between 1976 and 2017

| Migration Years | Total Migration |
|---|---|
| 1976–1981 | 46,992 |
| 1988–1993 | 80,368 |
| 2002–2007 | 74,531 |
| 2012–2017 | 61,542 |

Migration data collected from the Institute Nacional de Estadística y Informática (INEI).

*4.1.1 Population Growth and Migration.* Census data collected between 1940 and 2017 reveals a 1,048% increase in La Libertad's urban population as well as a 37% increase in the province's rural population (INEI n.d.). Despite the net increase of the rural population since 1940, the population actually declined by 13% between 2007 and 2017 (the most recent census years). Within the same decade, the urban population increased by 18%. Census data collected in 1972, 1981, 1993, 2007, and 2017 provides further insight into the decades spanning the current study (Table 5). The growth within the urban population occurred consistently between 1972 and 1981 (33%), 1981 and 1993 (37%), and 1993 and 2007 (36%). Migration to La Libertad has also contributed to population growth (Table 6). Domestic migrants, drawn by perceived economic opportunities, established residential communities in Trujillo's desert periphery in the early 1970s. The majority of this urbanization extended to the north and west of the city center [Gamboa 2016; Rosner 1997]. Known as *asentamientos humanos*, these urban communities were largely autonomous until their legal registration by district governments in the 1980s that brought water, electricity, and sewage connections [Gamboa 2016]. Peak immigration was recorded between 1988 and 1993 with 80,368 individuals relocating to La Libertad [INEI 2017b]. The consistent growth of Trujillo's urban population has accelerated the city's expansion and the concomitant destruction of archaeological sites. This is evident when comparing the overall increase in urban land use and the number of sites located in urban areas between 1985 and 2020 (Figure 2 and Table 3).

Population growth has continued to be a significant factor propelling housing demand and urban expansion. According to the Institute of Construction and Development of the Peruvian Chamber of Construction, construction in Trujillo grew by 500% between 2006 and 2012, with 84% of activity attributed to housing [RPP 2012]. As a response to rapid land development, archaeological survey prior to construction is now legally required in Peru [Higueras 2008]. Modern communities situated on the urban periphery prefer "to situate their houses near archaeological sites, even in the presence of nearby areas apparently without archaeological remains, in order to avail themselves of construction materials." [Gamboa 2016, p. 327]. Archaeological sites also provide an advantageous position against the risk of flooding [Gamboa 2016] and may provide irrigation and water access if pre-Columbian canals are still in use. Until the early 2010s, the expansion of Trujillo's metropolitan periphery was locally driven with little state planning or interference [Gamboa 2016]. The high rate of archaeological site destruction in the lower Moche Valley reflects the prioritization of resources like housing, water, and food access. The conservation of archaeological heritage sites has understandably remained a lower priority in areas where these basic needs are not being met.

The growth of Trujillo's urban community parallels a 19% increase in agricultural land use. Consumer demand for agricultural products has led to the simultaneous expansion of cropland as a result of Trujillo's population growth. Equally significant is the impact of Peru's Agrarian Reforms (1970s) and government policies implemented by former president Alberto Fujimori (1990s) concerning agricultural land use, urban migration, and subsequent archaeological destruction.

*4.1.2 Government Policies and Commercial Expansion.* The Agrarian Reform Law implemented in 1969 by General Juan Velasco Alvarado (1968–1975), sought to replace large landholding estates and subsistence farms. Through the expropriation of landholdings that exceeded 150 ha along Peru's coast, state regulations, and a new ban on neo-feudalism, the Velasco government attempted to increase agricultural productivity and move toward social equity by redistributing land to peasant communities [Cant 2021]. In the 12 years following the Velasco government, 15,000 properties (8 million ha) were expropriated and redistributed to peasant farmers through state-run cooperatives [Savoy 2011]. The new agricultural system and state regulations ultimately contributed to a decline in agricultural production, a greater reliance on imported goods to meet domestic food demands and population growth, and an intense rural migration to urban centers like Trujillo, Lima, and Chiclayo. The growth of the urban population caused a decline in coastal farmland as urban areas expanded and negatively impacted water supplies that formerly supported agricultural production [Savoy 2011]. Figure 2 underscores land changes occurring toward the end the Agrarian Reform period. Agricultural land is reduced from 12,407 ha in 1985 to 12,182 ha in 1990 and is offset by the simultaneous growth of Trujillo's urban footprint from 4,786 ha in 1985 to 5,626 ha in 1990.

The decline of coastal agriculture at the expense of urban expansion was short lived in the lower Moche Valley. The free-market policies of President Alberto Fujimori (1990–2000) served to reverse the expropriation and redistribution policies of the Agrarian Reforms and supported the development of a private agro-export sector [Savoy 2011]. New policies were created to reorient the economy toward export-led growth, facilitate access to land and water resources, and maximize domestic agriculture and production [Schwarz et al. 2016; Crabtree 2002]. Two key laws enacted between 1990 and 2000 have had a lasting impact on Peru's economy and land use: the "Foreign Investment Promotion Law" [1991] led to the equal treatment of foreign and domestic investors and liberalized land markets, and the "Agricultural Sector Promotional Law 27360," introduced in 2000 and extended until 2021, reduced taxes for agricultural companies and lowered the cost of agricultural labor [Schwarz et al. 2016]. Peru's **free trade agreements** (**FTAs**) negotiated during this period also generated tremendous growth.

The policies initiated by Fujimori shifted land use in the lower Moche Valley as the laws benefited large-scale producers connected to foreign markets. Farmland surrounding Trujillo rebounded during this period and continued to expand into the early 21st century, reaching a maximum extent of 15,079 ha by 2015. The formation of new markets and increased agro-industrial development along Peru's coast created a temporary boom for the asparagus, avocado, blueberry, and newly emerging quinoa industries. Recently established companies (both domestic and international) in Trujillo and its surrounding districts brought technological improvements and increased production capacity at export-oriented processing plants [Bedoya-Perales et al. 2018]. For example, Danper (a joint Danish-Peruvian venture founded in 1991) is one of Peru's largest agricultural companies, specializing in asparagus, artichoke, grape, and avocado production with the majority of exports focused on the U.S. and Europe. Danper's first production site was originally located in Trujillo, Peru and occupied 5,000 ha—a large portion of which was formerly desert [IFU 2021].

### 4.2 Secondary Drivers of Site Destruction

Two secondary drivers are attributed to site destruction in the lower Moche Valley: Peru's historic heritage discourse and historic state-emphasized heritage values. Individuals, communities, and governments influence and shape landscapes over time to enhance the availability of valued resources, whether cultural, economic, or social [Tengberg et al. 2012]. Peru has increasingly invested in making archaeological heritage tourism a socioeconomic priority. Although the country has expanded its regional archaeological attractions, it has simultaneously intensified tourism to the Cuzco region. Marca Peru, the multiregional emphasis of the Qhapaq Nan properties, and the recent inscriptions of Caral-Supe [2009] and Chankillo [2021] on the UNESCO World Heritage list (and the addition of the Chachapoyas sites of the Utcubamba Valley (including Kuelap) to the tentative list) are all state investments away from Cusco. These newly promoted state sites all preference monumental architecture. While conceptions of Peru's heritage are beginning to change at the local, national, and international levels, the Inca archaeological landscape has historically been (and continues to be) Peru's primary cultural ecosystem service in terms of tourism revenue and traditional heritage values.

The re-discovery of Machu Picchu in 1911 by Hiram Bingham's Yale Peruvian Expedition brought worldwide attention to Cusco, Peru and the architectural grandeur of the former Inca Empire. Media outlets like *National Geographic Magazine* and *Harper's Magazine* were quick to publish images of Cusco's rich archaeological remains, with the earliest guidebooks appearing in the late 1920s. The creation of the *Boleto Turístico del Cusco* in 1978, further emphasized the significance of *monumental* Inca sites, with eight former Inca royal estates anchoring the tourist circuit. The historic city center of Cusco and Machu Picchu would both be named UNESCO World Heritage sites in 1983, increasing their branding as "must-see," highly valued heritage destinations. Further, Peru's 1999 Tourist Master Plan designated Cusco as a priority tourism development zone. The Inca past has also increasingly intertwined with national heritage discourse, with former President Alejandro Toledo holding a symbolic inauguration at Machu Picchu in 2001. Toledo's reason for holding the additional ceremony at Machu Picchu, largely reflects national historic sentiment that the Inca represent "the glory of [the Peruvian] past" [Reuters 2001]. Following Toledo's inauguration, the campaign, "Peru—Land of the Inca" was used throughout the early 2000s to attract international tourists [Baumhackl 2019]. National rhetoric tying Peruvian identity to the Inca past has caused Inca heritage to be historically valued above other cultural periods and has greatly influenced tourist expectations and perceptions of Peruvian heritage. The high value placed on large-scale, monumental Inca sites as part of Peru's national heritage discourse has partially resulted in the concurrent devaluation of small-scale sites and higher destruction rates, both in Cusco and regions where the Inca past is limited.

While it is difficult to link intangible cultural values to empirical data, high rates of archaeological destruction can be used to extrapolate cultural values. As Gamboa [2016] has stated "…the adult population of the urban periphery of Trujillo frequently varies between emerging expectations and *a low interest with respect to the history and value of the local archaeological sites*." (author's emphasis). The destruction of archaeological sites in the lower Moche Valley is not only a product of modern socioeconomic pressures and policies (see Subsection 4.1), and Peru's traditional Inca-centric and monumental heritage discourse (discussed above), but also a simultaneous state-directed emphasis on a few high-profile tourism sites coupled with a lower status lack of engagement with second-tier sites. In the lower Moche Valley, high-profile sites (i.e., primary tier) include the UNESCO World Heritage Site of Chan Chan and the colonial city center of Trujillo, Huaca de la Luna y Huaca del Sol, El Brujo, and Arco Iris. State emphasis of monumental archaeological sites as valued heritage affects local and regional engagement with lower-order archaeological sites (e.g., CCMVP sites). For example, the Chimú household settlement of Cerro la Virgen located 6 km from Chan Chan, has been exposed to illegal gravel quarrying since 2006 [Billman et al. 2020] and periods of illegal housing since 2017 [Andina 2019]. Despite the site's designation as a *zona intangible* by the former Instituto Nacional de Cultura [Resolución Directoral 082–INC] and initiatives to slow the destruction rate, the planned expansion of the Carlos Martinez de Pinillos de Huanchaco airport will demolish the site in a bid to increase tourism and economic growth in the region [La Republica 2021]. Historically, the rate of small-scale site destruction in the lower Moche Valley reflects a lack of engagement and state investment in lesser known, understudied second-tier sites *as heritage* in favor of the economic or practical advantages that land development may offer.

While the historic trend of site destruction is clear, significant work to rescue small-scale sites continues to occur in the Moche Valley as new resources are invested into research. The Universidad Nacional de Trujillo and the Instituto Nacional de Cultura (currently the Ministerio de Cultura de Perú) have undertaken rescue excavations at sites threatened by urban and agricultural expansion including the CCMVP identified sites of Huaca Vichanzao and Las Lomas, among other sites in the region [Gamboa 2016]. Billman and colleagues' research and partnerships with local communities in the middle Moche Valley have helped sustain and preserve archaeological sites that would have otherwise been destroyed [Billman et al. 2018]. Recent research conducted at the heavily damaged site of Huanchaquito-Las Llamas revealed the largest child and camelid sacrifice in the New World [Prieto et al. 2019]. Such investigations are significant to continue to shift domestic heritage values and discourse at the local and national level (and altering international perspectives of Peru's heritage landscape) and are vital to the future preservation of small-scale sites in the Moche Valley, including remaining CCMVP sites.

## 4.3 Study Limitations

*4.3.1 Database Discrepancies.* Small, unavoidable discrepancies exist within the CCMVP database. Twenty-two sites do not have site numbers and are only listed as "MV ??." The site numbers either could not be interpreted or could not be recovered from the original CCMVP field notes during digitization conducted as part of the MVASD. These sites can only be distinguished by their UTM coordinates. The MV ?? sites were included in the present analysis since land use and potential destruction could still be calculated based on site coordinates. The inclusion of CCMVP coordinates and a list of remaining sites have been deliberately withheld from publication to protect remaining sites.

*4.3.2 Limitations of Satellite Imagery.* The method presented in this study is not meant to be a replacement for archaeological survey. Rather, the method provides archaeologists, government agencies, and NGOs with a relatively quick and cost-effective approach (compared to resurveying) to determine what remains of historically surveyed archaeological landscapes (i.e., surveys more than 50 years old), or alternatively what has been destroyed and why. It is increasingly important for archaeologists to place regional datasets within the context of site preservation or destruction, especially if there are landscape changes already taking place prior to surveys. Without doing so, archaeologists risk biasing remaining sites as being representative of *all* that was formerly on the landscape. The approach outlined in the current study also accelerates the process of selecting sites for targeted excavation, conservation efforts, and provides a deeper understanding of land-use change and its impact on archaeological sites.

One limitation of this approach is that satellite images do not show what could remain preserved underground, instead cataloging the probability of surface destruction. The assignment of the "high," "medium," and "low" land-use destruction categories is meant to inform targeted excavation and future survey work. Future ground-validation would be needed to infer various levels of site degradation that cannot be determined using Landsat satellite imagery. Landsat resolution is too course (30 m). Environmental factors (i.e., extensive cloud cover) or the absence of satellite imagery for a given region (see **Landsat Global Archive Consolidation** (**LGAC**)) may prevent the successful use of this method in some global locations.

# 5 CONCLUSION

This study provides an innovative approach to assess "what's left" of historically surveyed archaeological landscapes and quantify archaeological site destruction. Remote sensing paired with machine learning algorithms like RF provide greater accuracy for land-use classification and the analysis of archaeological landscapes. Researchers can easily access open source, global 30-m resolution Landsat satellite imagery for remote sensing analysis through the USGS's Earth Explorer. Combined with free, open source software like QGIS, the method outlined here offers a cost-effective option (compared to resurveying or purchasing high-resolution satellite imagery) that can be implemented by researchers, NGOs, and government agencies worldwide. The integration of land change science within archaeological survey also provides knowledge of LULCC drivers as well as how and why archaeological sites are destroyed (or survive) over time.

Using Peru's lower Moche Valley as a case study, 477 archaeological sites recorded during the CCMVP were analyzed. Results indicate that less than a quarter of these sites remain on the modern landscape, with urbanization and agricultural expansion accounting for 94.7% of site destruction. Underlying the expansion of these two land-use classes are government policies that have spurred migration and population growth within La Libertad and the Trujillo region. The devaluation and historically low prioritization of second-tier archaeological sites has also played a significant role in site destruction. CCMVP sites represent a small fraction of the total number of archaeological sites in the Moche Valley. The incorporation of additional archaeological survey data from the Moche Valley and neighboring regions of La Libertad could reveal broader land-use patterns and would likely increase known rates of archaeological destruction. Understanding land-use patterns and the underlying drivers of land-use change is significant for future archaeological survey and conservation as well as socioeconomic development as Peru seeks to establish alternative heritage tourism routes along the North Coast.

## ACKNOWLEDGMENTS

Thank you to Patrick Mullins and Brian Billman who generously provided the digitized site locations from the CCMVP. Thank you also to my colleague Robby Valderrama for hiking multiple miles per day with me to ground-verify CCMVP sites in the Moche Valley. I am grateful to Patrick Mullins, Eugenio Arima, and Alan Covey for their feedback and comments on earlier versions of this work.

## REFERENCES

S. Adelabu, M. Onisimo, and A. Elhadi. 2015. Testing the reliability and stability of the internal accuracy assessment of random forest for classifying tree defoliation levels using different validation methods. *Geocarto International* 30, 7 (2015), 810–821.

A. Agapiou. 2021. Multi-temporal change detection analysis of vertical sprawl over Limassol City Centre and Amathus archaeological site in Cyprus during 2015–2020 using the Sentinel-1 sensor and the Google Earth engine platform. *Sensors* 21, 5 (2021), 1884.

N. Álvarez-Berríós, J. L'Roe, and L. Naughton-Treves. 2021. Does formalizing artisanal gold mining mitigate environmental impacts? Deforestation evidence from the Peruvian Amazon. *Environmental Research Letters* 16, 6 (2021), 064052.

Andina. 2019. Trujillo: Desalojan a Invasores de Sitio Arqueológico Cerro La Virgen. Retrieved October 15, 2021 from https://andina.pe/agencia/noticia-trujillo-desalojan-a-invasores-sitio-arqueologico-cerro-virgen-756063.aspx.

W. Apaz, P. Quiroz, and A. Julca-Otiniano. 2019. Characterisation of avocado and asparagus farms in the Chavimochic irrigation project in La Libertad, Peru. *Peruvian Journal of Agronomy* 3, 3 (2019), 91–103.

G. P. Asner and R. Tupayachi. 2017. Accelerated losses of protected forests from gold mining in the Peruvian Amazon. *Environmental Research Letters* 12, 9 (2017), 094004.

H. Baumhackl. 2019. Peru "Land of the Incas". A tourism destination on the rise. *Tourism & Hospitality Management* 7, 2 (2019), 95–116.

V. Bax, W. Francesconi, and A. Delgado. 2019. Land-use conflicts between biodiversity conservation and extractive industries in the Peruvian Andes. *Journal of Environmental Management* 232 (2019), 1028–1036.

N. S. Bedoya-Perales, G. Pumi, A. Mujica, E. Talamini, and A. Domingos Padula. 2018. Quinoa expansion in Peru and its implications for land use management. *Sustainability* 10, 2 (2018), 532.

B. R. Billman. 2002. Irrigation and the origins of the southern Moche state on the North Coast of Peru. *Latin American Antiquity* 13, 4 (2002), 371–400.

B. R. Billman, D. Bardolph, J. Hudson, and J. Briceño Rosario. 2020. Fisherman, farmer, rich man, poor man, weaver, *Parcialidad* chief? *Maritime Communities of the Ancient Andes*. G. Prieto, and D. H. Sandweiss (Eds.). University of Florida Press, Gainesville, 265–300.

B. R. Billman, J. B. Rosario, A. Boswel, E. Freedman, and B. G. Jave. 2018. Creación de programas sostenibles de preservación del patrimonio en comunidades rurales: Un estudio de caso del valle de Moche, Perú. In *III Congreso Internacional de Buenas Prácticas en Patrimonio Mundial: Macciones integrales: Mahón, Menorca*. Universidad Complutense de Madrid, 105–115.

L. Breiman. 2001. Random forests. *Machine Learning* 45 (2001), 5–32.

M. Bürgi, P. H. Verburg, T. Kuemmerle, and T. Plieninger. 2017. Analyzing dynamics and values of cultural landscapes. *Landscape Ecology* 32 (2017), 2077–2081.

A. Cant. 2021. *Land without Masters: Agrarian Reform and Political Change Under Peru's Military Government*. University of Texas Press, Austin.

A. Caramanica, Huaman L. Mesia, C. R. Morales, G. Huckleberry, L. J. B. Castillo, and J. Quilter. 2020. El Niño resilience farming on the north coast of Peru. *Proceedings of the National Academy of Sciences USA* 117, 39 (2020), 24127–24137.

J. Casana. 2020. Global-scale archaeological prospection using CORONA satellite imagery: Automated, crowd-sourced, and expert-led approaches. *Journal of Field Archaeology* 45, 1 (2020), 89–100.

G. Caspari. 2020. Mapping and damage assessment of "royal" burial mounds in the Siberian Valley of the Kings. *Remote Sensing* 12, 5 (2020), 773.

L. J. B. Castillo and S. Uceda Castillo. 2008. *The Moche of Northern Perú. Handbook of South American Archaeology*. H. Silverman and W. Isbell (Eds.). Springer Science & Business Media, New York, 707–730.

C. Chapdelaine. 2011. Recent advances in Moche archaeology. *Journal of Archaeological Research* 19, 2 (2011), 191–231.

L. S. Coben. 2014. Sustainable preservation: Creating entrepreneurs, opportunities, and measurable results. *Public Archaeology* 13, 1-3 (2014), 278–287.

J. Crabtree. 2002. The impact of neo-liberal economics on Peruvian peasant agriculture in the 1990s. *Journal of Peasant Studies* 29, 3-4 (2002), 131–161.

B. Cuca and D. G. Hadjimitsis. 2017. Space technology meets policy: An overview of Earth observation sensors for monitoring of cultural landscapes within policy framework for cultural heritage. *Journal of Archaeological Science: Reports* 14 (2017), 727–733.

E. Cunliffe. 2014. Remote assessments of site damage: a new ontology. *International Journal of Heritage in the Digital Era* 3, 3 (2014), 453–473.

R. A. Dawson, G. P. Petropoulos, L. Toulios, and P. K. Srivastava. 2020. Mapping and monitoring of the land use/cover changes in the wider area of Itanos, Crete, using very high resolution EO imagery with specific interest in archaeological sites. *Environment, Development and Sustainability* 22 (2020), 3433–3460. https://doi.org/10.1007/s10668-019-00353-0

C. Doyle, T. Beach, and S. Luzzadder-Beach. 2021. Tropical forest and wetland losses and the role of protected areas in northwestern Belize, revealed from Landsat and machine learning. *Remote Sensing* 13, 3 (2021), 379.

A. Dupeyron. 2021. Capturing the impacts of archaeology for development: Opportunities and challenges in evaluating the sustainable preservation initiative in Peru. *Progress in Development Studies* 21, 2 (2021), 161–180.

H. El Hajj. 2021. Interferometric SAR and machine learning: Using open source data to detect archaeological looting and destruction. *Journal of Computer Applications in Archaeology* 4, 1 (2021), 47–62.

A. Elfadaly, W. Attia, M. M. Qelichi, et al. 2018. Management of cultural heritage sites using remote sensing indices and spatial analysis techniques. *Survey Geophysics* 39 (2018), 1347–1377.

J. Caballero Espejo, M. Messinger, F. Román-Dañobeytia, C. Ascorra, L. F. Fernandez, and M. Silman. 2018. Deforestation and forest degradation due to gold mining in the Peruvian Amazon: A 34-year perspective. *Remote Sensing* 10, 12 (2018), 1903.

I. S. Farrington and C. C. Park. 1978. Hydraulic engineering and irrigation agriculture in the Moche Valley, Peru: *c*. A.D. 1250–1532. *Journal of Archaeological Science* 5, 3 (1978), 255–268.

M. J. F. Fowler. 2010. The first space photographs and the origins of satellite archaeology. *AARGnews* 41 (2010), 25–38.

J. Gamboa. 2016. Archaeological heritage at risk: Preservation, destruction and perspectives for pre-Columbian sites from the periphery of Trujillo, Peru. *Complutum* 27, 2 (2016), 315–322.

H. J. Geist and E. F. Lambin. 2002. Proximate causes and underlying driving forces of tropical deforestation: Tropical forests are disappearing as the result of many pressures, both local and regional, acting in various combinations in different geographical locations. *BioScience* 52, 2 (2002), 143–150.

V. H. Gutiérrez-Vélez, R. DeFries, M. Pinedo-Vásquez, M. Uriarte, C. Padoch, W. Baethgen, and Y. Lim. 2011. High-yield oil palm expansion spares land at the expense of forests in the Peruvian Amazon. *Environmental Research Letters* 6, 4 (2011), 044029.

S. Hecht. 2010. The new rurality: Globalization, peasants and the paradoxes of landscapes. *Land Use Policy* 27, 2 (2010), 161–169.

A. Higueras. 2008. Cultural heritage management in Peru: Current and future challenges. *The Handbook of South American Archaeology*. H. Silverman and W. H. Isbell (Eds.). Springer, New York, NY, 1073–1088.

R. E. Hughes, E. Weiberg, A. Bonnier, M. Finné, and J. O. Kaplan. 2018. Quantifying land use in past societies from cultural practice and archaeological data. *Land* 7, 1 (2018), 9.

G. Huckleberry, F. Hayashida, and J. Johnson. 2012. New insights into the evolution of an intervalley prehistoric irrigation canal system, North Coastal Peru. *Geoarchaeology* 27, 6 (2012), 492–520.

M. A. Huston. 2005. The three phases of land-use change: Implications for biodiversity. *Ecological Applications* 15, 6 (2005), 1864–1878.

IFU (International Fund for Developing Countries). Leading Peru's Export of Agricultural Crops. Retrieved September 1, 2021 from https://www.ifu.dk/en/case/leading-perus-export-of-agricultural-crops/.

INEI (Instituto Nacional de Estadistica e Informatica). (n.d.). Evolución de la Población Censada Urbana, Según Departamento, 1940, 1961, 1972, 1981, 1993, 2007 y 2017. Retrieved August 23, 2021 from https://www.inei.gob.pe/estadisticas/indice-tematico/poblacion-y-vivienda/.

INEI (Instituto Nacional de Estadistica e Informatica). 2017b. Migración Interna. Retrieved August 23, 2021 from https://www.inei.gob.pe/estadisticas/indice-tematico/poblacion-y-vivienda/.

B. Kalantar, N. Ueda, V. Saeidi, K. Ahmadi, A. A. Halin, and F. Shabani. 2020. Landslide susceptibility mapping: Machine and ensemble learning based on remote sensing big data. *Remote Sensing* 12, 11 (2020), 1737.

A. Karamitrou, F. Sturt, P. Bogiatzis, and D. Beresford-Jones. 2022. Towards the use of artificial intelligence deep learning networks for detection of archaeological sites. *Surface Topography: Metrology and Properties* 10, 4 (2022), 044001.

M. Kempft. 2019. The application of GIS and satellite imagery in archaeological land-use reconstruction: A predictive model? *Journal of Archaeological Science: Reports* 25 (2019), 116–128.

P. Kosok. 1965. *Life, Land, and Water in Ancient Peru: An Account of the Discovery, Exploration, and Mapping of Ancient Pyramids, Canals, Roads, Towns, Walls, and Fortresses of Coastal Peru with Observations of Various Aspects of Peruvian Life, Both Ancient and Modern*. Long Island University Press, New York.

Arun D. Kulkarni and Barrett Lowe. 2016. Random Forest Algorithm for Land Cover Classification. *Computer Science Faculty Publications and Presentations*.

La Republica. 2021. Trujillo: Culminan Soterrado de Cableado Eléctrico para Ampliar Aeropuerto. Retrieved October 15, 2021 from https://larepublica.pe/sociedad/2021/09/10/trujillo-culminan-soterrado-de-cableado-electrico-para-ampliar-aeropuerto-lrnd/.

E. F. Lambin and P. Meyfroidt. 2011. Global land use change, economic globalization, and the looming land scarcity. *Proceedings of the National Academy of Sciences USA* 108, 9 (2011), 3465–3472.

Y. Li, J. Ma, and Y. Zhang. 2021. Image retrieval from remote sensing big data: A survey. *Information Fusion* 67 (2021), 94–115.

N. J. D. Loughlin, F. E. Mayle, N. B. Nuñez Otaño, J. M. K. O'Keefe, N. A. Duncan, J. H. Walker, and B. S. Whitney. 2021. Insights into past land-use and vegetation change in the Llanos de Moxos (Bolivia) using fungal non-pollen palynomorphs, *Journal of Archaeological Science* 130 (2021).

N. Masini and R. Lasaponara. 2020. Recent and past archaeological looting by satellite remote sensing: Approach and application in Syria. *Remote Sensing for Archaeology and Cultural Landscapes*. D. Hadjimitsis et al. (Eds.). Springer Remote Sensing/Photogrammetry. Springer, Cham, 123–137.

C. J. Mackey. 1982. The Middle Horizon as viewed from the Moche Valley. *Chan Chan: Andean Desert City*. M. E. Moseley and K. C. Day (Eds.). University of New Mexico Press, Albuquerque, 321–331.

B. G. Mark, A. French, M. Baraer, M. Carey, J. Bury, K. R. Young, M. H. Polk, Wigmore, P. Lagos, R. Crumley, J. M. McKenzie, and L. Lautz. 2017. Glacier loss and hydro-social risks in the Peruvian Andes. *Global and Planetary Change* 159 (2017), 61–76.

P. Meyfroidt, E. F. Lambin, K.-H. Erb, and T. W. Hertel. 2013. Globalization of land use: Distant drivers of land change and geographic displacement of land use. *Current Opinion in Environmental Sustainability* 5, 5 (2013), 438–444.

W. C. Miller. 1957. Uses of aerial photographs in archaeological field work. *American Antiquity* 23, 1 (1957), 46–62.

MINCETUR–Ministerio de Comercio Exterior y Turismo, Peru. Sistem de Inteligencia Tuística: Llegada de Visitantes a Sitios Turísticos, Museos y Áreas Naturales Protegidas por el Estado. Retrieved June 28, 2021 from https://www.mincetur.gob.pe/centro_de_Informacion/.

C. Moise, D. N. Iulia, C. E. Mihalache, A. M. Lazar, A. L. Dedulescu, G. T. Rustoiu, I. C. Inel, and A. Badea. 2021. Remote sensing for cultural heritage assessment and monitoring: The case study of Alba Iulia. *Sustainability* 13, 3 (2021), 1406.

J. D. Moore and C. J. Mackey. 2008. The Chimú empire. *Handbook of South American Archaeology*. H. Silverman and W. H. Isbell (Eds.). Springer, New York, 783–807.

M. E. Moseley and C. J. Mackey. 1972. Peruvian settlement pattern studies and small site methodology. *American Antiquity* 37, 1 (1972), 67–81.

M. E. Moseley and A. Cordy-Collins. 1990. *The Northern Dynasties: Kingship and Statecraft in Chimor*. Dumbarton Oaks, Washington, DC.

M. E. Moseley. 2001. *The Incas and Their Ancestors: The Archaeology of Peru* (revised ed.). Thames and Hudson, New York.

M. Nebbia, F. Cilio, and B. Bobomulloev. 2021. Spatial risk assessment and the protection of cultural heritage in southern Tajikistan. *Journal of Cultural Heritage* 49 (2021), 183–196.

Q. H. Nguyen, H.-B. Ly, L. S. Ho, N. Al-Ansari, H. V. Le, V. Q. Tran, I. Prakash, and B. T. Pham. 2021. Influence of data splitting on performance of machine learning models in prediction of shear strength of soil. *Mathematical Problems in Engineering* (2021), 1–15.

M. Olivier and W. B. Verschoof. 2021. Implementing state-of-the-art deep learning approaches for archaeological object detection in remotely-sensed data: The results of cross-domain collaboration. *Journal of Computer Applications in Archaeology* 4, 1 (2021), 274–289.

H. A. Orengo, F. C. Conesa, A. Garcia-Molsosa, A. Lobo, A. S. Green, M. Madella, and C. A. Petrie. 2020. Automated detection of archaeological mounds using machine-learning classification of multisensor and multitemporal satellite data. *Proceedings of the National Academy of Sciences USA* 117, 31 (2020), 18240–18250.

C. R. Ortloff, R. A. Feldman, and M. E. Moseley. 1985. Hydraulic engineering and historical aspects of the pre-Columbian intravalley canal systems of the Moche Valley, Peru. *Journal of Field Archaeology* 12, 1 (1985), 77–98.

S. Parcak. 2015. Archaeological looting in Egypt: A geospatial view (case studies from Saqqara, Lisht, and el Hibeh). *Near Eastern Archaeology* 78, 3 (2015).

D. Plekhov, P. VanValkenburgh, P. Abrams, A. Cutler, J. Han, A. J. Reátegui Díaz, B. Sullivan, and S. Wernke. 2021. Linking past and present land-use histories in Southern Amazonas, Peru. *Remote Sensing* 13, 12 (2021), 2274.

G. Prieto, J. W. Verano, N. Goepfert, D. Kennett, J. Quilter, S. LeBlanc., L. Fehren-Schmitz, J. Forst, M. Lund, B. Dement, et al. 2019. A mass sacrifice of children and camelids at the Huanchaquito-Las Llamas site, Moche Valley, Peru. *PLoS One* 14, 3 (2019), e0211691. https://doi.org/10.1371/journal.pone.0211691

J. Quilter. 2021. Moche pottery: Forms, functions, and social change. *Ñawpa Pacha* 41 2 (2021), 187–209.

A. Rahman, H. M. Abdullah, T. Tanzir, J. Hossain, B. M. Khan, G. Miah, and I. Islam. 2020. Performance of different machine learning algorithms on satellite image classification in rural and urban setup. *Remote Sensing Applications: Society and Environment* 20 (2020), 100410.

E. Ráez Luna. 2017. *En medio de avalanchas e inundaciones, Perú se enfrenta a décadas de desarrollo irregular.* New York Times. Retrieved June 23, 2021 from https://www.nytimes.com/es.

A. Ramirez, A. Pacheco, and J. Telles. 2019. Mapping vegetation, water bodies and urban areas in PeruSAT-1 satellite imagery. In *2019 XXII Symposium on Image, Signal Processing and Artificial Vision (STSIVA'19)*. 1–4.

L. Rayne, J. Bradbury, D. Mattingly, G. Philip, R. Bewley, and A. Wilson. 2017. From above and on the ground: Geospatial methods for recording endangered archaeology in the Middle East and North Africa. *Geosciences* 7, 4 (2017), 100.

R. R. Rindfuss, S. J. Walsh, B. L. Turner II, J. Fox, and V. Mishra. 2004. Developing a science of land change: Challenges and methodological issues. *Proceedings of the National Academy of Sciences USA* 101, 39 (2004), 13976–13981.

W. Rosner. 1997. Migration and the development of an industrial district: Footwear manufacturing in El Porvenir, Trujillo-Peru. *Yearbook (Conference of Latin Americanist Geographers)* 23 (1997), 107–117.

RPP Noticias. 2012. Actividad Constructora creció en 500% en Trujillo. Retrieved June 23, 2021 from https://rpp.pe/peru/actualidad/actividad-constructora-crecio-en-500-en-trujillo-noticia-487281.

T. K. Rudel, R. Defries, G. P. Asner, and W. F. Laurance. 2009. Changing drivers of deforestation and new opportunities for conservation. *Conservation Biology* 23, 6 (2009), 1396–1405.

A. M. Sánchez-Cuervo, L. S. de Lima, F. Dallmeier, P. Garate, A. Bravo, and H. Vanthomme. 2020. Twenty years of land cover change in the southeastern Peruvian Amazon: implications for biodiversity conservation. *Regional Environmental Change* 20 (2020), 1–14.

S. Savoy. 2011. Law's Labor's lost: Failure of Peru's 1969 Agrarian reform law to stimulate agricultural production. *Border-Lines: Journal of the Latino Research Center* 5 (1969), 14–44.

J. Schwarz, M. Schuster, B. Annaert, M. Maertens, and E. Mathijs. 2016. Sustainability of global and local food value chains: An empirical comparison of Peruvian and Belgian asparagus. *Sustainability* 8, 4 (2016), 344.

J. Schwarz and E. Mathijs. 2017. Globalization and the sustainable exploitation of scarce groundwater in coastal Peru. *Journal of Cleaner Production* 147 (2017), 231–241.

M. Schuster and M. Maertens. 2016. Do private standards benefit workers in horticultural export chains in Peru? *Journal of Cleaner Production* 112 (2016), 2392–2406.

I. Shimada. 2000. The late prehispanic coastal states. *The Inca World: The Development of Pre-Columbian Peru AD 1000–1534,* L. Laurencich Minelli (Eds.). University of Oklahoma Press, Norman, 49–64.

L. Stephens, D. Fuller, N. Boivin, T. Rick, N. Gauthier, A. Kay, B. Marwick, C. G. Armstrong, C. M. Barton, and T. Denham, et al. 2019. Archaeological assessment reveals Earth's early transformation through land use. *Science* 365, 6456 (2019), 897–902.

K. Tatsumi, Y. Yamashiki, A. K. M. Morante, L. R. Fernandez, and R. A. Nalvarte. 2016. Pixel-based crop classification in Peru from Landsat 7 ETM+ images using a Random Forest model. *Journal of Agricultural Meteorology* 72, 1 (2016), 1–11.

A. E. Thompson. 2020. Detecting classic maya settlements with lidar-Derived relief visualizations. *Remote Sensing* 12, 17 (2016), 2838.

A. Tengberg, S. Fredholm, I. Eliasson, I. Knez, K. Saltzman, and O. Wetterberg. 2012. Cultural ecosystem services provided by landscapes: Assessment of heritage values and identity. *Ecosystem Services* 2 (2012), 14–26.

D. Tewabe and T. Fentahun. 2020. Assessing land use and land cover change detection using remote sensing in the Lake Tana Basin, Northwest Ethiopia. *Cogent Environmental Science* 6, 1 (2020), 1778998.

B. L. Turner, E. F. Lambin II, and A. Reenberg. 2007. The emergence of land change science for global environmental change and sustainability. *Proceedings of the National Academy of Sciences USA* 104, 52 (2007), 20666–20671.

N. M. Underberg-Goode. 2014. Cultural heritage tourism on Peru's North Coast. *Worldwide Hospitality and Tourism Themes* 6, 3 (2014), 200–214.

P. Van Valkenburgh, K. C. Cushman, L. J. C. Butters, C. R. Vega, C. B. Roberts, C. Kepler, and j. Kellner. 2020. Lasers without lost cities: Using drone lidar to capture architectural complexity at Kuelap, Amazonas, Peru. *Journal of Field Archaeology* 45, sup1 (2020), S75–S88.

C. Vargas, J. Montalban, and A. A. Leon. 2019. Early warning tropical forest loss alerts in Peru using Landsat. *Environmental Research Communications* 1, 12 (2019), 121002.

E. Vaz. 2020. Archaeological sites in small towns—a sustainability assessment of Northumberland County. *Sustainability* 12, 5 (2018).

L. A. Vega Isuhuaylas, Y. Hirata, L. C. Ventura Santos, and N. Serrudo Torobeo. 2018. Natural forest mapping in the Andes (Peru): A comparison of the performance of machine-learning algorithms. *Remote Sensing* 10, 5 (2018), 782.

F. G. Velarde. 2018. Land struggles in vulnerable coastal territories: Tourism development in Mancora, Peru. *Tijdschrift voor Economische en Sociale Geografie* 110, 1 (2018), 70–82.

M. A. Vogel. 2018. New research on the late prehistoric coastal polities of Northern Peru. *Journal of Archaeological Research* 26 (2018), 165–195. https://doi.org/10.1007/s10814-017-9108-0

J. Wang, Y. Zheng, M. Wang, Q. Shen, and J. Huang. 2021. Object-scale adaptive convolutional neural networks for high-spatial resolution remote sensing image classification. *IEEE Journal of Selected Topics in Applied Earth Observation and Remote Sensing* 14 (2021), 283–299.

S. Wernke, P. VanValkenburgh, and A. Saito. 2020. Interregional archaeology in the age of big data: Building online collaborative platforms for virtual survey in the Andes. *Journal of Field Archaeology* 45, 1 (2020), 61–74.

G. Willey. 1953. Prehistoric Settlement in the Virú Valley, Peru. Washington: United States Government Printing Office.

World Bank. 2021. Chavimochic Irrigation Project-Peru. Updated May 3, 2021. Accessed June 28, 2021 from https://ppp.worldbank.org/public-private-partnership/library/chavimochic-irrigation-project-peru.

N. E. Young, R. S. Anderson, S. M. Chignell, A. G. Vorster, R. Lawrence, and P. H. Evangelista. 2017. A survival guide to Landsat preprocessing. *Ecology* 98, 4 (2017), 920–932.

C. Zarro, S. L. Ullo, G. Meoli, and M. Focareta. 2020. Semi-automatic classification of building from low-density Lidar data and Worldview-2 images through OBIA technique. In *Proceedings of the 2020 IEEE International Geoscience and Remote Sensing Symposium (IGARSS'20)*. 992–995.

K. S. Zimmerer and H. L. R. Vaca. 2016. Fine-grain spatial patterning and dynamics of land use and agrobiodiversity amid global changes in the Bolivian Andes. *Regional Environmental Change* 16 (2016), 2199–2214.

I. Zingman, D. Saupe, O. A. Penatti, and K. Lambers. 2016. Detection of fragmented rectangular enclosures in very high resolution remote sensing images. *IEEE Transactions on Geoscience and Remote Sensing* 54, 8 (2016), 4580–4593.

Received 13 July 2022; revised 8 December 2022; accepted 26 December 2022